◆ Human Brain Mapping 35:3216–3226 (2014) ◆

Quantification of Primary Motor Pathways Using Diffusion MRI Tractography and Its Application to Predict Postoperative Motor Deficits in Children With Focal Epilepsy

Jeong-Won Jeong,* Eishi Asano, Csaba Juhász, and Harry T. Chugani

Carman and Ann Adams Department of Pediatrics, Department of Neurology, School of Medicine, Wayne State University, Detroit, Michigan, USA
Translational Imaging Laboratory, Children's Hospital of Michigan, Detroit, Michigan, USA

Abstract: As a new tool to quantify primary motor pathways and predict postoperative motor deficits in children with focal epilepsy, the present study utilized a maximum *a posteriori* probability (MAP) classification of diffusion weighted imaging (DWI) tractography combined with Kalman filter. DWI was performed in 31 children with intractable focal epilepsy who underwent epilepsy surgery. Three primary motor pathways associated with "finger," "leg," and "face" were classified using DWI-MAP classifier and compared with the results of invasive electrical stimulation mapping (ESM) via receiver operating characteristic (ROC) curve analysis. The Kalman filter analysis was performed to generate a model to determine the probability of postoperative motor deficits as a function of the proximity between the resection margin and the finger motor pathway. The ROC curve analysis showed that the DWI-MAP achieves high accuracy up to 89% (finger), 88% (leg), 89% (face), in detecting the three motor areas within 20 mm, compared with ESM. Moreover, postoperative reduction of the fiber count of finger pathway was associated with postoperative motor deficits involving the hand. The prediction model revealed an accuracy of 92% in avoiding postoperative deficits if the distance between the resection margin and the finger motor pathway seen on preoperative DWI tractography was 19.5 mm. This study provides evidence that the DWI-MAP combined with Kalman filter can effectively identify the locations of cortical motor areas even in patients whose motor areas are difficult to identify using ESM, and also can serve as a reliable predictor for motor deficits following epilepsy surgery. *Hum Brain Mapp 35:3216–3226, 2014.* © 2013 Wiley Periodicals, Inc.

Key words: primary motor pathway; corticospinal tract; diffusion weighted image tractography; presurgical planning; epilepsy

INTRODUCTION

The principle of presurgical evaluation for epilepsy is to determine the spatial relationship between the epileptogenic zone and functionally important ("eloquent") cortex [Rosenow and Luders, 2001]. Without accurate localization of such brain regions, one cannot secure the ultimate goal of epilepsy surgery, which is to resect the epileptic tissue without creating a new sensorimotor or cognitive deficit. The most vital structures to be preserved include the

Contract grant sponsor: National Institutes of Health; Contract grant numbers: R01 NS064033, R01 NS041922, R01 NS064989

*Correspondence to: Jeong-Won Jeong, Departments of Pediatrics and Neurology, Wayne State University School of Medicine, PET Center, Children's Hospital of Michigan, 3901 Beaubien Blvd, Detroit, MI 48201. E-mail: jeongwon@pet.wayne.edu

Received for publication 4 March 2013; Revised 21 June 2013; Accepted 2 August 2013.

DOI 10.1002/hbm.22396
Published online 18 October 2013 in Wiley Online Library (wileyonlinelibrary.com).

primary cortical motor areas and underlying motor pathways.

The gold-standard method to define the primary motor areas is electrical stimulation mapping (ESM) via subdural electrodes implanted on the brain surface [Lesser et al., 2010; Wylle and Awad, 1991]. However, ESM is not an ideal diagnostic modality, because of its insensitivity to find the motor areas in young children [Chitoku et al., 2001; Haseeb et al., 2007; Wylle and Awad, 1991]. A previous study reported that no contralateral hand movement was elicited by electrical stimulation in 15 of 65 children, and that the average age of these 15 patients was 3.4 years [Haseeb et al., 2007]. Inevitable limitations of ESM also include sampling errors; for example, the primary motor leg area is difficult to localize by ESM, unless subdural electrodes are placed exactly on the cortical tissues of interest in the interhemispheric fissure. An alternative approach to localize hand motor areas is functional MRI (fMRI). However, fMRI is highly susceptible to movement artifacts and demands cooperative behaviors during scanning; thus, its success rate in young children is limited [Berntsen et al., 2008; de Ribaupierre et al., 2012; Grabski et al., 2012; Rumpel et al., 2009; Wengenroth et al., 2011]. Indeed, proportional success rate for the completion of an individual fMRI run in children with epilepsy was reported to be $60 \pm 5\%$ at ages of 4–6 years [Yerys et al., 2010], suggesting limited applicability of fMRI to young children with epilepsy.

To overcome the limitations of ESM and fMRI, our recent study applied independent component analysis combined with ball and stick model (ICA+BSM) tractography [Jeong et al., 2012, 2013a] to achieve an automatic classification of different primary motor pathway segments, called a maximum *a posteriori* probability (MAP) classifier [Jeong et al., 2013b], which can automatically detect three important pathways of "finger," "leg," and "face" areas from both corticobulbar tracts (CBT) and corticospinal tracts (CST), based on their stereotaxic atlases constructed from healthy children. Compared with fMRI and ESM, this method achieved high accuracy to detect correct locations of "finger," "leg," and "face" areas derived from clinical diffusion weighted imaging (DWI) data [Jeong et al., 2013a,b]. The proposed method does not require patient cooperation and can be ultimately applied to other pathways in infants and young children in whom localization of the primary motor cortex is difficult using fMRI or ESM. fMRI studies also involve an additional cost, whereas the proposed DWI approach can be acquired as a part of the clinical MRI. Therefore, validation using the clinical outcome is warranted to determine if this can be considered as a reliable noninvasive, alternative imaging method for planning surgical intervention in young children with focal epilepsy. The specific goals of the present study were: (1) to assess whether the DWI-MAP classifier can delineate the primary motor pathways of "finger," "leg," and "face" whose ESM failed to detect motor sites in children with epilepsy, (2) to assess whether the DWI-MAP can delineate primary motor areas of "finger," "leg," and "face" in the vicinity of structural lesions, (3) to quantify the baseline of motor function in "finger," "leg," and "face" before surgical resection, and (4) to develop a new clinical model combining "DWI-MAP classifier" with "Kalman filter" [Hamilton, 1994] for prediction of postoperative motor deficits and for defining the optimal safety margin of resection to avoid postoperative motor deficits. We expect that this new paradigm, if validated, will have a significant impact on the clinical management of epileptic patients whose epileptogenic zone is in close proximity to the motor pathways.

METHODS

Study Subjects

Thirty-one children with a diagnosis of focal epilepsy (age: 8.3 ± 6.9 years, 0.7–17.1 years, 16 boys) were investigated in this study. All participants were right-handed. None of the patients had significant hemiplegia. Some patients had minor fine motor deficits but gross motor function was preserved in all patients before surgery. Fifteen children had structural lesions within the rolandic region or a gyrus immediately adjacent to it on neuroimaging. The 31 patients were selected by using the following inclusion criteria: (i) a history of intractable focal epilepsy scheduled for extraoperative subdural ESM as a part of presurgical evaluation at Children's Hospital of Michigan, Detroit, (ii) mapping of motor and sensory functions via ESM. The exclusion criteria consisted of: (i) history of gross motor deficits, (ii) history of previous neurological surgery, and (iii) presence of massive brain malformations (such as large perisylvian polymicrogyria or hemimegalencephaly which entirely eliminate the anatomical landmarks for the central sulcus and sylvian fissure); these patients usually undergo one-stage hemispherectomy without extraoperative electrocorticography recording in our institute. Patients with other lesions including focal cortical dysplasia, cortical tubers, brain tumor, gliosis, and inflammation were not excluded from this study.

All study participants received a set of preoperative evaluations, such as clinical assessment of gross motor performance and MRI scans, while 13 participants had the same evaluations after epilepsy surgery. Post-operative motor impairment, presence or absence of newly developed gross motor deficit, was assessed clinically by a pediatric neurologist at the time of post-operative MRI scan. All studies were performed in accordance with policies of the Wayne State University Institution Review Board with written informed consent.

Data Acquisition

MRI scans were performed on a 3T GE-Signa scanner (GE Healthcare, Milwaukee, WI) equipped with an 8-channel head coil and ASSET. Pre- and post-operative

DWI data were acquired as a part of the clinical MRI, with a multi-slice single shot diffusion weighted echo-planar-imaging (EPI) sequence at TR = 12,500 ms, TE = 88.7 ms, FOV = 24 cm, 128x128 acquisition matrix (nominal resolution = 1.89 mm), contiguous 3 mm thickness in order to cover entire axial slices of whole brain using 55 isotropic gradient directions with $b = 1{,}000$ s/mm^2, one $b = 0$ acquisition, and number of excitations (NEX)=1. Approximate scanning time for this acquisition was about 12 min using double refocusing pulse sequence to reduce eddy current artifacts. For anatomical reference, three-dimensional fast spoiled gradient echo sequence (FSPGR) was acquired for each participant at TR/TE/TI of 9.12/3.66/400 ms, slice thickness of 1.2 mm, and planar resolution of 0.94×0.94 mm^2.

Extraoperative Electrocorticography and Electrical Stimulation Mapping (ESM)

All patients underwent subdural electrode placement as a part of the clinical management for medically uncontrolled seizures. Extraoperative electrocorticography was obtained, and the seizure onset zones were clinically determined in each case [Asano et al., 2009].

ESM, using the method previously established [Fukuda et al., 2008; Haseeb et al., 2007], was performed as part of the clinical care during extraoperative electrocorticography recordings. A pair of subdural electrodes was stimulated by an electrical pulse-train of 5-s maximum duration using pulses of 300 μs duration and frequency of 50 Hz. Initially, stimulus intensity was set to 3 mA. Stimulus intensity was increased from 3 to 9 mA in a stepwise manner by 3 mA increments until a clinical response or after-discharge on electrocorticography was observed. When an after-discharge without an observed clinical response, or when neither a clinical response nor an after-discharge was induced by the maximally intense stimuli, the site was declared "not proven eloquent". When both a clinical response and after-discharges occurred, another pulse-train of the same or 1 mA smaller intensity was used until either a clinical response or an after-discharge failed to develop. Cortical regions underlying electrodes whose stimulation induced a contralateral movement, without after-discharges, were defined as "the primary motor areas" for a given body part: finger, leg, and face. Those sites were spatially registered to MRI space [Fukuda et al., 2008] and then used as the ground-truth for the comparison with DWI-MAP classification.

Cortical resection was guided mainly by ictal and interictal extraoperative electrocorticography, as well as neuroimaging data [Asano et al., 2009]. We generally intended to remove all of the seizure onset zones in most of the patients. When the seizure onset zones were close to or within the eloquent cortex such as the ESM-defined sensorimotor area, the extent of cortical resection was determined after the epilepsy surgery team and the family of

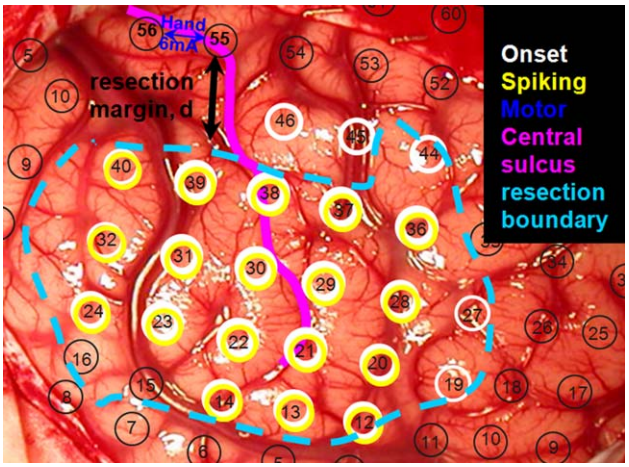

Figure 1.
An example of ESM to determine epileptogenic zone (cyan), finger area (blue), and resection margin, d (black). Black circles indicate an array of subdural electrodes placed on the brain. [Color figure can be viewed in the online issue, which is available at wileyonlinelibrary.com.]

the patient had extensive discussions regarding the pros and cons of surgical resection of such areas. The resection margin was marked and documented using intraoperative pictures taken before and immediately after the resection (Fig. 1).

DWI-MAP Classification to Detect Primary Motor Pathways

Details of DWI-MAP classifier were reported in our recent study [Jeong et al., 2013b]. For each participant, whole brain ICA+BSM tractography was performed to reconstruct white matter fibers, $f_j(x,y,z)$ in the CBT/CST pathways. To classify individual fibers, $f_j(x,y,z)$ into one of the following four classes (i.e., C_1: mouth/lip CBT, C_2: finger CST, C_3: leg CST, C_4: other remaining CBT/CST), stereotaxic MNI probability maps of four CBT/CST pathways, $P(x,y,z \mid C_{i=1,2,3,4})$ were placed into the participant's head space by applying the inverse of spatial deformation obtained between the subject's b0 image and MNI b0 template [Ashburner, 2007; Jeong et al., 2013b]. Under equal priors for four classes, $C_{i=1,2,3,4}$, this study assumes that *a posteriori* probability of a fiber $f_j(x,y,z)$ to belong to a class C_i, $P(f_j \mid C_i)$, is equal to an average value of $P(x,y,z \mid C_i)$ over the entire trajectory of $f_j(x,y,z)$.

$$P(f_j|C_i) = \frac{1}{N}\sum_x \sum_y \sum_z f_j(x,y,z) P(x,y,z|C_i) \qquad (1)$$

where $P(x,y,z \mid C_i)$ represents a stereotaxic probability map of class C_i in native head space obtained via inverse

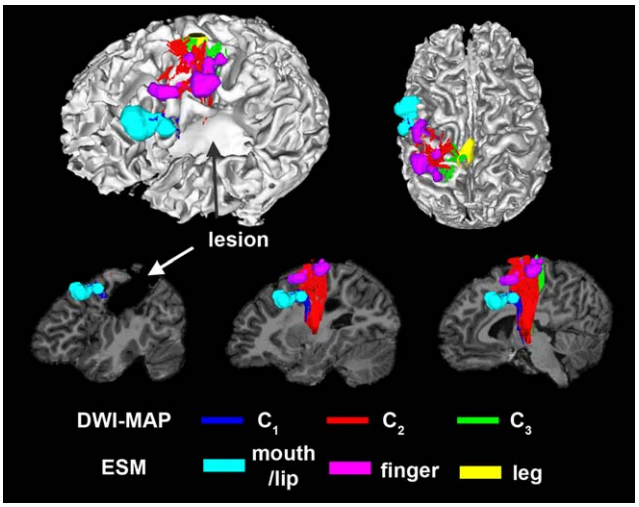

Figure 2.

Automatic detection of three pathways using the DWI-MAP classifier, C_1: mouth/lip (blue), C_2: finger (red), C_3: leg (green) obtained from 9 years old child with focal epilepsy and a lesion involving the pre/post-central gyrus. The ESM sites of mouth/lip (cyan), finger (pink), and leg (yellow) were compared with C_1, C_2, and C_3 of DWI-MPA classifier, respectively. [Color figure can be viewed in the online issue, which is available at wileyonlinelibrary.com.]

spatial normalization of a standard atlas, $P(x,y,z \mid C_i)$ mapping from MNI b0 template to the subject's b0 image [Ashburner, 2007]. The value of $f_j(x,y,z)$ is equal to a unit when fiber f_j intersects a point (x,y,z). N indicates the total number of intersections. Since the present study assumes an equal prior of C_i for $i = 1,2,3,4$, the argument of i having the maximum posteriori probability, $P(f_j \mid C_i)$, determines the class membership of a given fiber, f_j.

Figure 2 shows an example of DWI-MAP classification obtained from a patient with a lesion involving the primary motor area in the precentral gyrus. It is apparent that the DWI-MAP classifier can delineate three motor pathways near the lesion. Since the DWI-MAP classifier refers to probabilistic values of individual CST/CBT fibers ranging from the internal capsule to cortex, it has the ability to detect CST/CBT pathways that are partially deviated to an unpredicted direction due to a lesion located in the region of these pathways.

Comparison of DWI-MAP Classification With ESM

To train an optimal DWI-MAP classification and avoid a circular analysis in comparing the DWI-MAP classification with ESM, we employed a systematic "leave-one-out" trial approach where M-whole brain tracts, $f_{j=1,2,\ldots,M}$, of a single subject was classified into one of four classes, $C_{i=1,2,3,4}$, by instantaneous DWI-MAP classifier whose $P(x,y,z \mid C_{i=1,2,3,4})$ was learned on the remaining subjects in the same group [Jeong et al., 2013b]. At each trial, the cortical points of individual fibers, f_j, in C_i defined functional areas of C_i determined by DWI-MAP. Areas of DWI-MAP were compared with their gold standard, ESM grid electrode locations for children with focal epilepsy, with a match considered to occur if areas of DWI-MAP contacted and overlapped areas of the gold standard. Matches between the DWI-MAP and the gold standard were also assessed as a function of distance to estimate receiver operating characteristic (ROC) curves [FitzGerald et al., 1997; Jeong et al., 2013a,b]. The borders of DWI-MAP areas ($C_{i=1,2,3}$) were extended by 5, 10, 15, and 20 mm to determine whether the number of matches changed. The sensitivity, specificity, and accuracy of $C_{i=1,2,3}$ were assessed in each subject, separately. Finally group averaging of accuracy, sensitivity, and specificity for $C_{i=1,2,3}$ was performed for all possible leave-one-out trials.

Kalman Filter Analysis to PredictMotorDeficit and Optimal Resection Margin

The present study introduces the theory of Kalman filter [Hamilton, 1994] to determine an optimal margin of resection to avoid postoperative motor deficits and determine the probability of motor deficits as a function of distance between the motor pathways and the resection margin. We assume that the resection margin, d, is a dynamic variable to control the state vector, $x(d)$, affecting the postoperative change in fiber count, $y(d)$, where the linear dynamic system models a stochastic process with linear dynamics: $x(d)$, and linear observation: $y(d)$.

$$x(d+1)=F^{*}x(d)+w(d), w \sim N(0,Q), x(0) \sim N(x(0),V(0))$$
$$y(d)=H^{*}x(d)+v(d), v \sim N(0,R) \quad (2)$$

where $x(d)$ is the hidden state at a given margin, d and $y(d)$ is the observation, which is the reduced extent of fiber count after the surgery. F and H indicate system matrix and observation matrix in the linear dynamic model, respectively. Q, R, and v represent system covariance, observation covariance, and state covariance, respectively. $N(\mu,\Sigma)$ indicates white Gaussian noise with mean, μ, and covariance, Σ.

The Kalman filter is known as a linear quadratic estimation to learn the conditional probability of $P(x(d) \mid y(1),y(2),\ldots,y(d))$ via expectation maximization. By referering to ESM and DWI-MAP, both d and $y(d)$ are observed after the surgery. These two variables are then utilized to estimate the hidden state vector, $x(d)$ in Eq. (3). To obtain a better estimate of $y(d)$ in a relatively smaller sample size, this study utilizes the Rauch-Tung-Striebel (RTS) algorithm [Rauch et al., 1965], which performs fixed-interval offline smoothing. Finally, an optimal margin, d_{opt}, securing no loss of fibers, is found at $y(d_{opt})=0$. The probability of postoperative motor deficit

at a given margin (d): P(deficit | d) is estimated by the following equation:

$$P(\text{deficit}\,|d)=1-\int_0^d \beta(d)dd,$$
$$\text{where}\ \beta(d)=\frac{\alpha(d)}{\int_0^\infty \alpha(d)dd},\ \alpha(d)=y(d)-\min\,(y(d)) \quad (3)$$

where $\beta(d)$ represents a cummerative density function of $\alpha(d)$ defining the measurement $y(d)$ corrected with its minimal value, min($y(d)$).

RESULTS

Accuracy of DWI-MAP Classifier in Children With Focal Epilepsy

The DWI-MAP classifier showed that the cortical areas of C_1 (mouth/lip), C_2 (finger), and C_3 (leg), were mainly localized at or near the pre/post-central gyrus, and these DWI-defined areas apparently matched well to those of the gold-standard ESM in 31 children with epilepsy (Fig. 3). The ROC curves of sensitivity, specificity, and accuracy of data are shown in Figure 4. Using leave-one-out cross validation, the sensitivity of the DWI-MAP over ESM increased from 36% (mouth/lip), 59% (finger), 60% (leg) to 94% (mouth/lip), 100% (finger), and 100% (leg), respectively, as the criterion changed from "contact" to "20 mm away from the center of the electrode". The specificity of the DWI-MAP classifier decreased from 98% (mouth/lip), 96% (finger), 97% (leg) to 87% (mouth/lip), 80% (finger), 84% (leg) as the criterion was relaxed from "contact" to "20 mm from the tracts to the center of the electrode". The DWI-MAP provided high accuracy for the CST fibers terminating in proximity to the localization of ESM, 77% for mouth/lip, 76% for fingers, 86% for leg (contact), and 89% for mouth/lip, 89% for finger, 88% for leg (within 20 mm).

The ROC analyses obtained from age-gender matched two groups of children with focal epilepsy, i.e., group 1 (G_1): focal epilepsy with no lesion (n=16), and group 2 (G_2): focal epilepsy with lesion (n=15) are presented in Figure 5. Comparable accuracy was found in $C_1/C_2/C_3$ of the two groups (G_1: 77%/77%/83% and G_2: 77%/75%/88% at the criterion of contact), suggesting that DWI-MAP classifier can detect the three motor pathways without being affected by the presence of structural lesions.

Postoperative Change in Fiber Count Measured by DWI-MAP Classifier

Figure 6 presents representative examples of C_2 (finger) where preoperative and postoperative DWI-MAP classifications were compared in two children with focal epilepsy. In the first child, the resection of the presumed epileptogenic zone in the right frontal lobe yielded no postoperative loss of the finger pathway. In the second

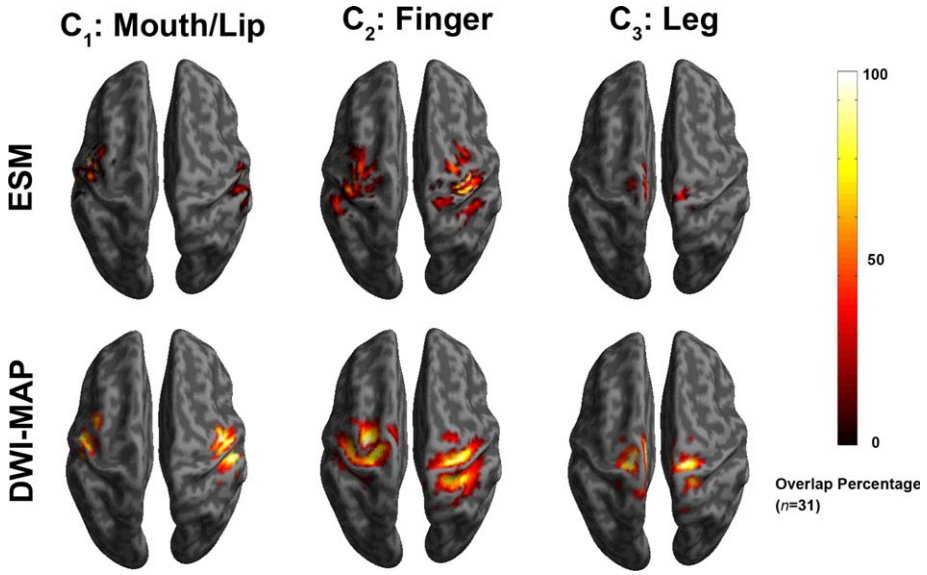

Figure 3.

Comparison of overlap percentage maps obtained from ESM (top) and DWI-MAP classification (bottom) in children with epilepsy (n = 31). Both ESM and DWI-MAP of individual subjects were spatially transferred into standard MNI space and overlapped across subjects. Color bar indicates the overlap percentage of all cortical localizations obtained by each modality. [Color figure can be viewed in the online issue, which is available at wileyonlinelibrary.com.]

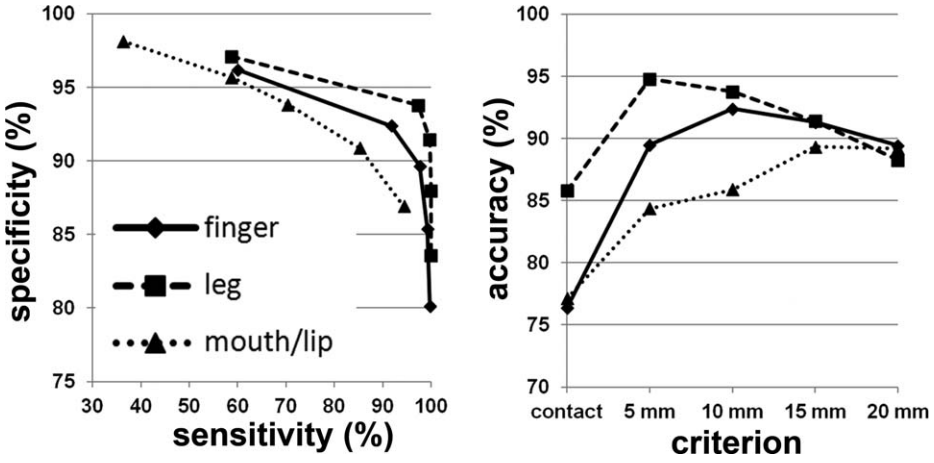

Figure 4.

Receiver operator curve analyses for the three pathways, C_1: mouth/lip (▲), C_2: finger (◆), and C_3: leg (■). For each of five separation criteria (contact, 5 mm, 10 mm, 15 mm, 20 mm), the group average of sensitivity, specificity, and accuracy was evaluated from children with focal epilepsy ($n = 31$).

child, the resection of the right hemispheric cortex including a brain tumor resulted in a marked loss of the finger pathway, yielding significantly reduced CST fibers in the right hemisphere on postoperative MRI (because the tumor involved most of primary motor area at the central sulcus).

Postoperative fiber count changes in C_2 (finger) were analyzed in 13 children with focal epilepsy, all of who had no presurgical motor impairment (Fig. 7). Six of the 13 children suffered from postoperative hand motor deficits. All seven children with no postoperative hand motor deficits showed no change or even slightly increased fiber count in C_2 (finger), indicating intact (and normally developing) CST fibers. Conversely, five of the six children in the group with new postoperative motor deficit showed significantly reduced fiber counts in C_2 of DWI-MAP classification, suggesting that the proposed DWI-MAP can effectively quantify postsurgical motor deficits.

Prediction of Postoperative Hand Motor Deficit and Optimal Resection Margin Using Kalman Filter

By adapting the theory of Karma filter in Eq. (2), it was found that fiber count of C_2 (finger) increased exponentially as a function of resection margin. An optimal margin, securing no loss of fibers (or no associated motor deficit), d_{opt}, was found at 19.5 mm (Fig. 8). Notably, there were no patients who suffered postoperative weakness when resection was done beyond this optimal margin.

The probability of motor deficit in C_2 (finger), estimated by using Eqs. (2) and (3), quadratically decreased as the resection margin increased (Fig. 9). The probability of motor deficit, $p(\text{deficit} \mid d = d_{opt})$ in the finger pathway was approximately predicted at the range of 0.5 ± 0.061, implying that when the resection margin from ESM finger site (d) is determined at $d_{opt} = 19.5$ mm, there is an even chance to yield a postoperative motor deficit in the finger.

Table I shows how accurately the obtained optimal margin predicted avoiding postoperative motor deficits. Based on Fisher's exact probability test [Agresti, 1992], ESM cases satisfying $d \geq d_{opt}$ yielded 100% of no postoperative deficit while the ones satisfying $d < d_{opt}$ yielded 86% of motor deficit (P-value of Fisher's exact test = 0.004). Kalman filter provided high true positive rate (0.86), low false positive rate (0) and high accuracy (0.92) to predict an optimal margin, d_{opt} ensuring no motor deficit.

To demonstrate how reliably the proposed Kalman filter predicts the probability of postoperative motor deficit in clinical practice, safe limits of finger CST denoting discrete probabilities of motor deficit, $p(\text{deficit} \mid d = 0$ mm,10 mm,20 mm) were separately drawn on the structural MRI of one patient (Fig. 10). It is clear in this case that the narrow limit, predicting greater than 80% chance of deficit, included the lesion (which was resected), indicating a high chance to have postoperative deficit if the entire lesion was removed. In fact, the resection of this lesion caused severe motor impairment of the contralateral fingers.

DISCUSSION

Three major findings emerge from the present study. First, the proposed DWI-MAP classifier can accurately delineate three important CST pathways associated with "finger," "leg," and "face," that invasive ESM procedure failed to localize in some children with focal epilepsy. The ROC curve analysis showed that the DWI-MAP achieved high accuracy, up to 89% (mouth/lip), 89% (finger), and 88% (leg) in automatically detecting three CST pathways

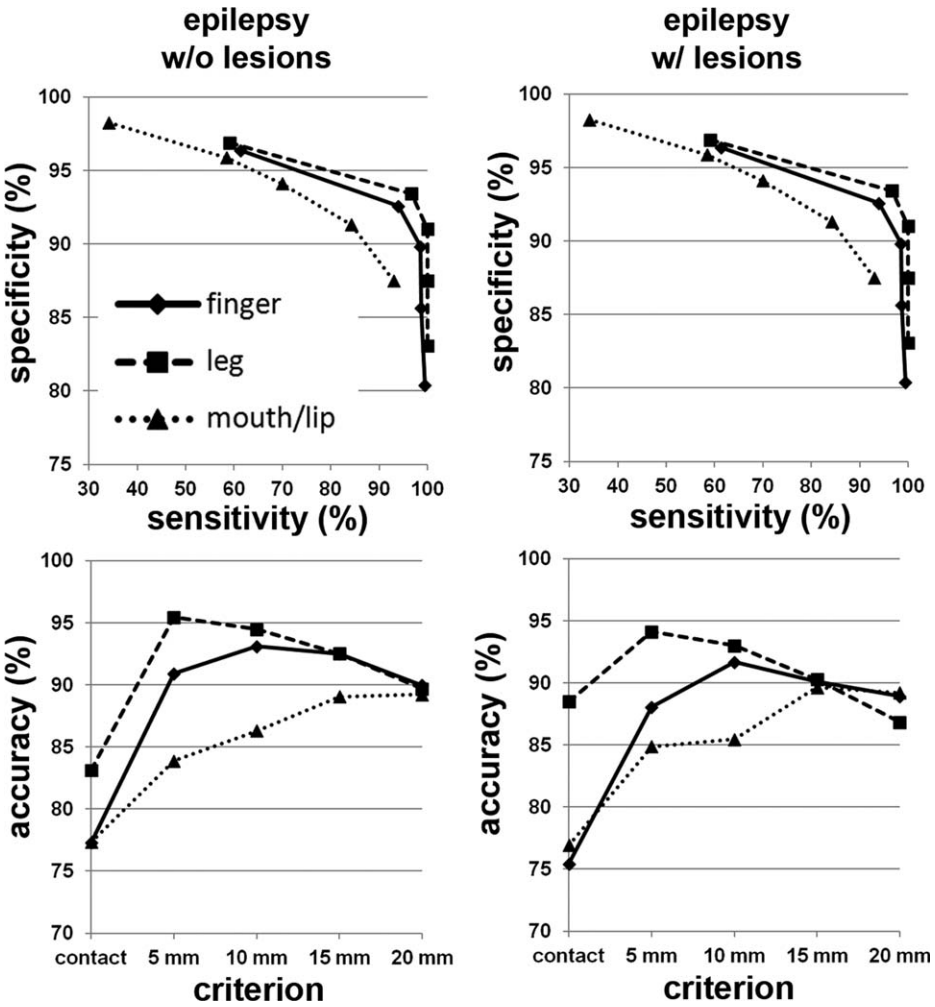

Figure 5.

Receiver operator curve analyses for the three pathways, C_1: mouth/lip (▲), C_2: finger (◆), and C_3: leg (■). For each of five separation criteria (contact, 5 mm, 10 mm, 15 mm, 20 mm), the group average of sensitivity, specificity, and accuracy was evaluated from epilepsy children without lesion (left column, $n=16$) and with lesion (right column, $n=15$).

within 2 cm. Second, the postoperative deficit in motor function was associated with postoperative reduction of CST fiber count on DWI data. By comparing fiber count of finger pathway between pre-/post-operative measurements, this study showed that postoperative decrease in fiber count of the finger pathway results in postoperative motor deficit of the hand/finger. This finding suggests that postsurgical motor outcome may substantially differ according to the extent of resected white matter encompassing the CST, and DWI-MAP classifier can improve the prediction of motor outcome. This result clearly substantiates our hypothesis that the DWI-MAP classifier can monitor postoperative motor deficits. Third, the proposed Kalman filter analysis determined the probability of motor deficit as a function of surgical resection margin determined by the ESM procedure. As demonstrated in 13 children with focal epilepsy, an optimal margin securing no motor deficit in finger was found when the resection margin was set to be 19.5 mm, leading to 100% of no postoperative deficit at the margin $\geq$ 19.5 mm and 86% of motor deficit at the margin $<$ 19.5 mm. This could be an important reference for clinical practice in planning the resection margin for preservation of vital motor functions in epilepsy surgery.

Several studies have reported the feasibility of using DWI at the early stage of neurosurgical planning and follow-up to predict and manage motor deficit after surgical treatment [Kovanlikaya et al., 2011; Laundre et al., 2005; Puig et al., 2010]. However, those studies have been limited to assess the medial part of the CST associated

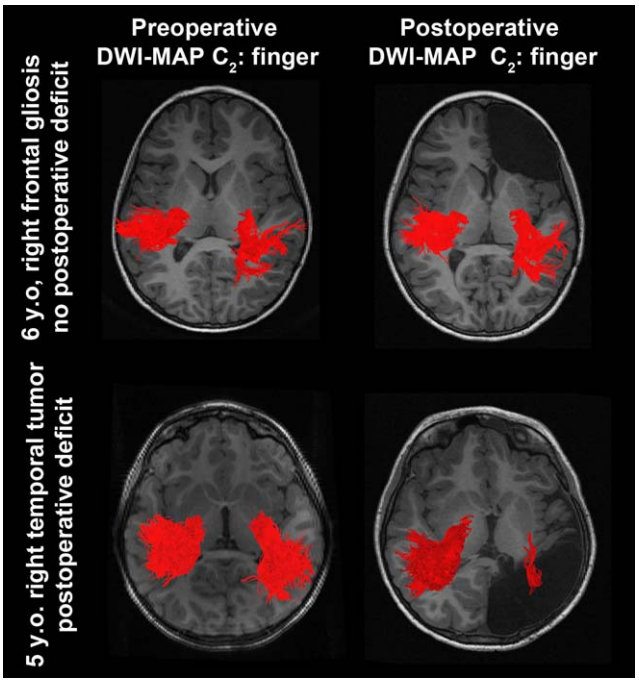

Figure 6.

Representative examples of C_2 (finger) pathways (red fibers) obtained from preoperative DWI-MAP classifier (left column) and postoperative DWI-MAP classifier (right column). The resection of the presumed epileptogenic zone in the right frontal lobe yielded no loss of the finger pathway (top); in contrast, the resection of the right hemisphere including a tumor resulted in significant loss of the finger pathway (bottom). [Color figure can be viewed in the online issue, which is available at wileyonlinelibrary.com.]

mostly with motor function of the leg and trunk due to the intravoxel crossing fiber problem [Jeong et al., 2012; Qazi et al., 2009; Singh et al., 2010]. By adapting ICA+BSM tractography into the DWI-MAP classifier, the present study could effectively demarcate lateral projections of CST to assess motor functions associated with "finger" and "face". This has an important implication to monitor primary motor functions in many pediatric neurological disorders such as Sturge-Weber syndrome (SWS) with common cortical/subcortical pathology in the vicinity of the sensori-motor area [Bodensteiner and Roach, 2010; Riela and Roach, 2004]. Conventional MRI during the early disease course often provides false assurance by showing a normal brain or underestimating brain damage in young children with SWS who later develop signs of motor deficits [Lo et al., 2012]. By performing longitudinal studies to monitor the changes in fiber counts of individual segments for finger, leg, and face, it will become possible to assess the severity of cortical and white matter injury affecting specific motor functions and predict subsequent motor deficits in young children with SWS and other pathologies in the vicinity of the motor pathways.

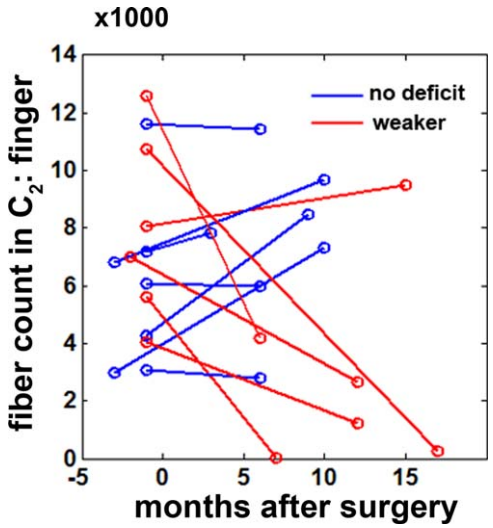

Figure 7.

Fiber counts in C_2 (finger) of two different DWI data obtained from before and after surgery ($n = 13$, 7 children with no postoperative motor deficit and 6 children who developed postoperative hand motor impairment). The month of surgery is indicated by 0. [Color figure can be viewed in the online issue, which is available at wileyonlinelibrary.com.]

DWI tractography of structural lesions requires careful consideration of data analysis to avoid the effect of pseudo-diffusion created by slow blood flow in the lesion capillary

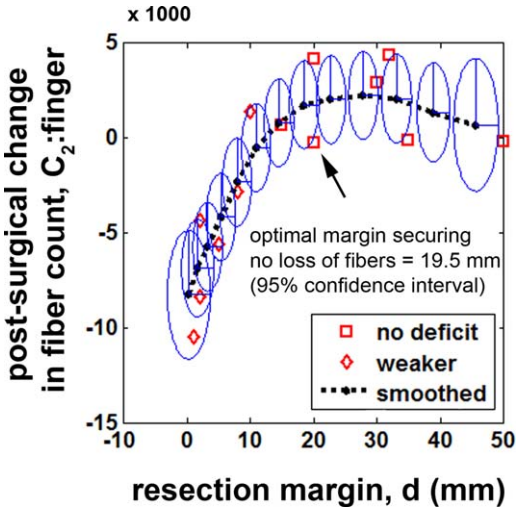

Figure 8.

Prediction of postsurgical change in C_2: finger regressed by Eq. (2). Interval changes in fiber count, |presurgical C_2: finger - postsurgical C_2: finger|, of thirteen children who had no preoperative motor deficit were plotted with the corresponding resection margins. Eclipses represent uncertainties at 95% confidence. [Color figure can be viewed in the online issue, which is available at wileyonlinelibrary.com.]

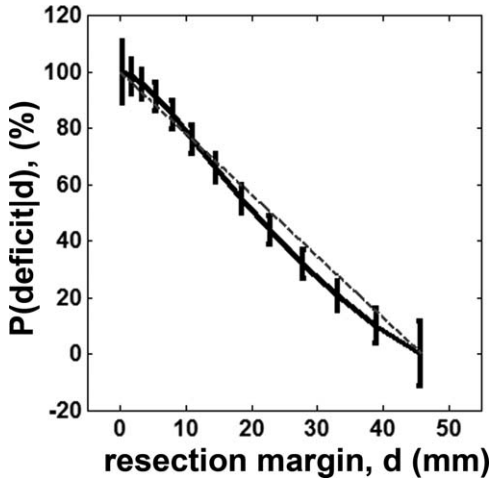

Figure 9.

Probability of finger motor deficit at a given resection margin. The value of P(deficit|d) was converted to % by multiplying 100 to that of Eq. (3). Vertical bars indicate ±one standard deviations scaling the degree of uncertainty at the resection margin.

bed, probably increasing isotropic components in DWI signals. As reported in our previous study [Jeong et al., 2012], the ICA+BSM has an isotropic ball compartment, which can comprehensively model water diffusivity in lesion tissue, leading to better accuracy to resolve the orientations of CST in the vicinity of a structural lesion. Furthermore, the DWI-MAP classifier refers to probabilistic values of individual CST/CBT fibers, $P(x,y,z \mid C_{i=1,2,3,4})$, ranging from internal capsule to cortex, suggesting that it may readily detect CST/CBT pathways deviated to an unpredicted direction due to a lesion located in the region or vicinity of these pathways. Nonetheless, this study assumes that no significant reorganization takes place in the development of CST pathways in children with focal epilepsy having structural lesion. Also, postoperative motor deficits in neurosurgery are not only caused by removal of the brain tissue but can also be caused by ischemic lesions. The early sign of ischemic changes could have been seen on early postoperative DWI scan, which was not available in most patients

TABLE I. 2 × 2 contingency table in 13 surgical patients where d_{opt} was applied to predict the finger motor deficit

	$d \geq d_{opt}$	$d < d_{opt}$	Total (n)
No deficit	6	1	7
Deficit	0	6	6
Total (n)	6	7	13

*Fisher's exact probability test [Agresti, 1992] was performed for 2 × 2 contingency table (P-value of Fisher's exact test = 0.004). True positive rate (0.86), false positive rate (0) and accuracy (0.92) were obtained to predict an optimal margin, d_{opt} ensuring no motor deficit.

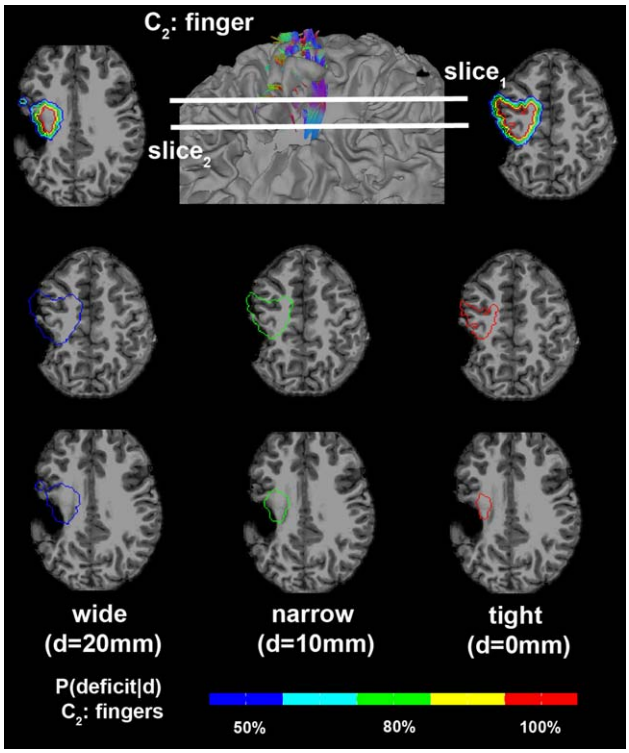

Figure 10.

Safe limits to preserve finger CST defined by discrete resection margins predicting the probability of motor deficit, P(deficit|d) in Figure 9. Three boundaries at the margins of d = 0 mm, 10 mm, and 20 mm were overlaid to MRI of a 9-year-old child with epilepsy and structural lesion. Each colored contour indicates the safe limit to avoid the color-coded value of P(deficit|d). [Color figure can be viewed in the online issue, which is available at wileyonlinelibrary.com.]

included in this study. In addition, comparing ESM with the DWI-MAP classifier, it is notable that the ESM showed less overlap percentage than DWI-MAP classifier, especially in C_1 (face) and C_3 (leg). ESM had a greater failure rate to detect the areas of face and leg, due to patient fatigue and sampling errors, which may limit its comparison with DWI-MAP classifier to identify the tracts associated with face and leg areas. Future studies should carefully investigate how the performance of DWI-MAP classifier is affected by those confounds: size and location of ischemic lesions, reorganization, and lower sensitivity of ESM in patients with focal epilepsy.

The ideal goal of epilepsy surgery is to maximize the resection of the epileptogenic zone and minimize postoperative motor deficit by avoiding unnecessary resection of primary motor areas. While a 1 cm margin has been shown to result in significantly fewer language deficits [FitzGerald et al., 1997], and 8 mm was reported as the largest preoperatively measured tumor-to-tract distance with a positive stimulation result [Zolal et al., 2012], there has been no

quantitative study for children with epilepsy to predict the probability of motor deficits in terms of the resection margin. The proposed Kalman analysis found a relatively greater margin, 19.5 mm, to avoid severe postoperative motor deficit under 50% of probability. A significant nonlinear pattern was observed between the resection margin and the probability of motor deficit. Although this optimal margin and pattern was estimated from a limited sample-size, the findings of this study might be useful to facilitate an objective benefit-risk analysis. Future studies will thoroughly investigate the variations of this optimal margin and pattern in larger groups and across developmental ages.

CONCLUSIONS

To overcome clinical limitation of fMRI and ESM in children with focal epilepsy, this study investigated whether DWI-MAP classifier combined with Kalman filter analysis can be an effective alternative of fMRI and ESM to localize three important motor areas ("finger," "leg," "face") and predict postoperative motor deficit after epilepsy surgery in children. The results demonstrated that the proposed method could be clinically useful for presurgical planning in young children who cannot follow task instructions for fMRI and are insensitive to electrical stimulations in ESM procedure. Moreover, the proposed method can be used to optimize resection margin preserving vital axonal pathways by predicting the probability of postoperative motor deficit as a function of resection margin determined by the ESM procedure.

ACKNOWLEDGMENTS

The authors would like to thank all participants and their families for their time and interest in this study. The authors declare no conflicts of interest.

REFERENCES

Agresti A (1992): A survey of exact inference for contingency tables. Statistical science 7:131–153.

Asano E, Juhász C, Shah A, Sood S, Chugani HT (2009): Role of subdural electrocorticography in prediction of long-term seizure outcome in epilepsy surgery. Brain 132(Part 4):1038–1047.

Ashburner J (2007): A fast diffeomorphic image registration algorithm. Neuroimage 38:95–113.

Berntsen EM, Samuelsen P, Lagopoulos J, Rasmussen IA Jr, Håberg AK, Haraldseth O (2008): Mapping the primary motor cortex in healthy subjects and patients with peri-rolandic brain lesions before neurosurgery. Neurol Res 30:968–973.

Bodensteriner JB, Roach ES (2010): Sturge-Weber syndrome, The Sturge-Weber Foundation, New York: Mt. Freedom. pp 19–32.

Chitoku S, Otsubo H, Harada Y, Jay V, Rutka JT, Weiss SK, Abdoll M, Snead OC III (2001): Extraoperative cortical stimulation of motor function in children. Pediatr Neurol 24:344–350.

de Ribaupierre S, Fohlen M, Bulteau C, Dorfmüller G, Delalande O, Dulac O, Chiron C, Hertz-Pannier L (2012): Presurgical language mapping in children with epilepsy: Clinical usefulness of functional magnetic resonance imaging for the planning of cortical stimulation. Epilepsia 53:67–78.

FitzGerald DB, Cosgrove GR, Ronner S, Jiang H, Buchbinder BR, Belliveau JW, Rosen BR, Benson RR (1997): Location of language in the cortex: A comparison between functional MR imaging and electrocortical stimulation. Am J Neuroradiol 18: 1529–1539.

Fukuda M, Nishida M, Juhász C, Muzik O, Sood S, Chugani HT, Asano E (2008): Short-latency median-nerve somatosensory-evoked potentials and induced gamma-oscillations in humans. Brain 131:1793–1805.

Grabski K, Lamalle L, Vilain C, Schwartz JL, Vallée N, Baciu M, Le Bas JF, Sato M (2012): Functional MRI assessment of orofacial articulators: Neural correlates of lip, jaw, larynx, and tongue movements. Hum Brain Mapp 33:2306–2321.

Hamilton JD. 1994. Time Series Analysis. New Jersey: Princeton University Press. pp 372–408.

Haseeb A, Asano E, Juhász C, Shah A, Sood S, Chugani HT (2007): Young patients with focal seizures may have the primary motor area for the hand in the postcentral gyrus. Epilepsy Res 76:131–139.

Jeong JW, Asano E, Yeh FC, Chugani DC, Chugani HT (2012): Independent component analysis tractography combined with ball and stick model to isolate intra-voxel crossing fibers of the corticospinal tracts in clinical diffusion MRI. Mag Reson Med Sep 21. doi:1.1002/mrm.24487 [Epub ahead of print].

Jeong JW, Chugani HT, Juhasz C (2013a): Localization of primary motor cortex segments using white matter connectivity between precentral gyrus and posterior limb of internal capsule: A multimodal imaging analysis. J Magn Reson Imaging Mar 5. doi:10.1002/jmri.24076. [Epub ahead of print].

Jeong JW, Asano E, Brown EC, Tiwari VN, Chugani DC, Chugani HT (2013b): Automatic detection of primary motor areas using diffusion MRI tractography: Comparison with functional MRI and electrical stimulation mapping. Epilepsia Jun 17. doi: 10.1111/epi.12199. [Epub ahead of print].

Kovanlikaya I, Firat Z, Kovanlikaya A, Ulug AM, Cihangiroglu MM, John M, Bingol CA, Ture U (2011): Assessment of the corticospinal tract alternations before and after resection of brainstem lesions using Diffusion Tensor Imaging (DTI) and tractography at 3T. Eur J Radiol 77:383–391.

Laundre BJ, Jellison BJ, Badie B, Alexander AL, Field AS (2005): Diffusion tensor imaging of the corticospinal tract before and after mass resection as correlated with clinical motor findings: Preliminary data. Am J Neuroradiol 26:791–796.

Lesser RP, Crone NE, Webber WR (2010): Subdural electrodes. Clin Neurophysiol 121:1376–1392.

Lo W, Marchuk DA, Ball KL, Juhasz C, Jordan LC, Ewen JB, Comi A (2012): Updates and future horizons on the understanding, diagnosis, and treatment of Sturge-Weber syndrome brain involvement. Dev Med Child Neurol 54:214–223.

Oldfield RC (1971): The assessment and analysis of handedness: The Edinburgh inventory. Neuropsychologia 9:97–113.

Puig J, Pedraza S, Blasco G, Baunis-I-Estadella J, Prats A, Prados F, Boada I, Castellanos M, Sanchez-Gonzalez J, Remollo S, Laguillo G, Quiles AM, Gomez E, Serena J (2010): Wallerian degeneration in the corticospinal tract evaluated by diffusion tensor imaging correlates with motor deficit 30 days after middle cerebral artery ischemic stroke. Am J Neuroradiol 31:1324–1330.

Qazi AA, Radmanesh A, O'Donnell L, Kindlmann G, Peled S, Whalen S, Westin CF, Golby AJ (2009): Resolving crossings in the corticospinal tract by two-tensor streamline tractography:

Method and clinical assessment using fMRI. Neuroimage 47(Suppl 2):T98–T106.
Rauch HE, Tung F, Striebel CT (1965): Maximum likelihood estimates of linear dynamic systems, AIAA J3:1445–1450.
Riela AR, Roach ES (2004): Sturge-Weber syndrome, In: Roach ES, Miller VS, editors. Neurocutaneous Disorder. New York: Cambridge University Press. pp 179–195.
Rosenow F, Lűders H. 2001. Presurgical evaluation of epilepsy. Brain 124(Part 9):1683–1700.
Ruge MI, Victor J, Hosain S, Correa DD, Relkin NR, Tabar V, Brenna C, Gutin PH, Hirsch J (1999): Concordance between functional magnetic resonance imaging and intraoperative language mapping. Stereotact Funct Neurosurg 72:95–102.
Rumpel H, Chan LL, Tan JS, Ng IH, Lim WE (2009): Clinical functional magnetic resonance imaging for pre-surgical planning—The Singapore General Hospital experience with the first 30 patients. Ann Acad Med Singapore 38:782–786.
Schlosser MJ, Luby M, Spencer DD, Awad IA, McCarthy G (1999): Comparative localization of auditory comprehension by using functional magnetic resonance imaging and cortical stimulation. J Neurosurg 91:626–635.
Singh M, Wong CW (2010): Independent component analysis-based multifiber streamline tractography of the human brain. Magn Reson Med 64:1676–1684.
Wengenroth M, Blatow M, Guenther J, Akbar M, Tronnier VM, Stippich C (2011): Diagnostic benefits of presurgical fMRI in patients with brain tumours in the primary sensorimotor cortex. Eur Radiol 21:1517–1525.
Wyllie E, Awad I (1991): Invasive neurophysiologic techniques in the evaluation for epilepsy surgery in children. In: Luders HO, editor. Epilepsy Surgery. New York: Raven Press. pp 409–412.
Yerys BE, Jankowski KF, Shook D, Rosenberger LR, Barnes KA, Berl MM, Ritzl EK, VanMeter J, Vaidya CJ, Gaillard WD (2010): The fMRI success rate of children and adolescents: Typical development, epilepsy, attention deficit/hyperactivity disorder, and autism spectrum disorders. Hum Brain Mapp 30: 3426–3435.
Zolal A, Hejčl A, Vachata P, Bartoš R, Humhej I, Malucelli A, Nováková M, Hrach K, Derner M, Sameš M (2012): The use of diffusion tensor images of the corticospinal tract in intrinsic brain tumor surgery: A comparison with direct subcortical stimulation, Neurosurgery 71:331–340.